Numerical simulation of Josephson traveling-wave parametric amplifier

FACULTY OF MATHEMATICS, PHYSICS AND INFORMATICS
Comenius University Bratislava

Emil Rizvanov, Samuel Kern, Pavol Neilinger and Miroslav Grajcar

Department of Experimental Physics, Comenius University, SK-84248 Bratislava, Slovakia

Let's connect on LinkedIn :)

Introduction

Traveling-wave parametric amplifiers (TWPAs) are essential tools for ultrasensitive measurements, particularly in superconducting quantum computing. Achieving high gain and broad bandwidth requires careful dispersion engineering, typically through the incorporation of resonant elements along the transmission line or periodic modulation of its parameters. These structures exhibit complex nonlinear wave interactions that can either enhance or suppress amplification. Understanding these processes and their influence on amplifier performance is essential for optimizing TWPA designs. To investigate these processes, we combine time-domain simulations in JoSIM and WRspice with analytical coupled-mode theory. High-performance computing enable extensive parameter sweeps to systematically investigate nonlinear effects and identify designs and operating conditions that provide high gain and broad bandwidth. The designs, verified by numerical simulations, will be tested in our dilution refrigerator at temperatures down to 10 mK.

TWPAs as Quantum-Limited Amplifiers

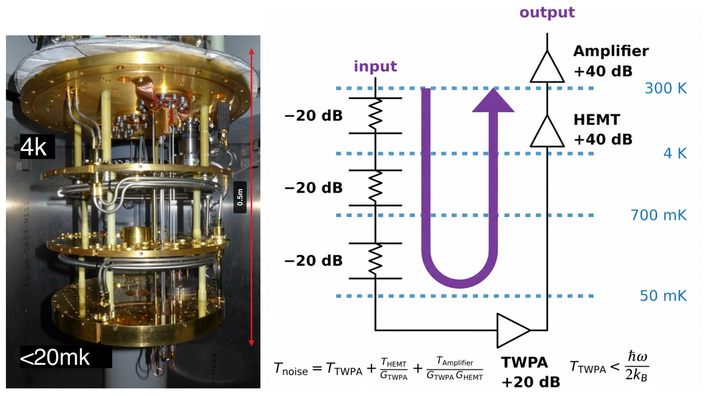


Figure 1: TWPA noise temperature can be an order of magnitude lower than that of HEMT amplifiers. Consequently, utilizing a Josephson amplifier with an amplification exceeding 10 dB as a preamplifier enables reducing the cryogenic HEMT amplifier's noise temperature.

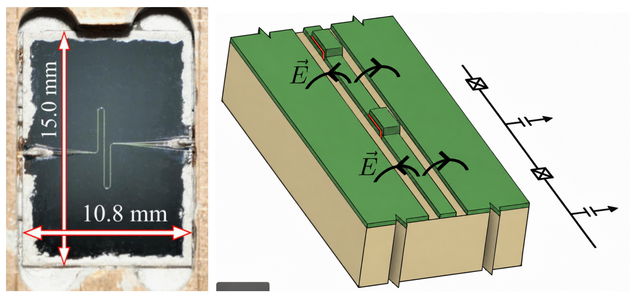


Figure 2: A TWPA can be viewed as a continuous nonlinear medium. Nevertheless, the device is implemented as a discrete chain of Josephson junctions. Because the physical length of a single junction cell ($l_{JJ} = 5\ \mu$m) much smaller than and the wavelength of relevant operating frequencies ($f \lesssim 10$ GHz).

Coupled mode theory predicts high broadband gain for phase-matched waves

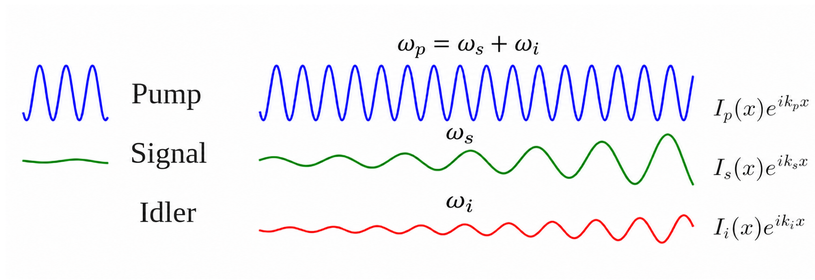


Figure 3: propagating waves

$$v_p^2 \frac{\partial^2 I(x,t)}{\partial x^2} - \frac{\partial^2 I(x,t)}{\partial t^2} = \frac{\partial^2}{\partial t^2}\left(\frac{1}{2}\epsilon I(x,t)^2 + \frac{1}{3}\xi I(x,t)^3\right) \quad (1)$$

$$G(L) = \cosh^2(gL) + \left(\frac{\beta}{2g}\right)^2 \sinh^2(gL) \quad (2)$$

$$g = \sqrt{\frac{k_s k_i}{4}\left(\frac{I_p I_d}{I_d^2 + I_*^2}\right)^2 - \frac{\beta^2}{4}}, \quad (3)$$

nonlinear phase shift per unit length

$$\beta = \Delta k\left(1 + \frac{I_p^2}{4(I_d^2 + I_*^2)}\right) - \frac{I_p^2}{8(I_d^2 + I_*^2)} k_p, \Delta k = k_p - k_s - k_i \quad (4)$$

- In uniform TWPAs, achievable gain is limited.
- In order to maximize the gain, the phase matching should be achieved $\beta = 0$.

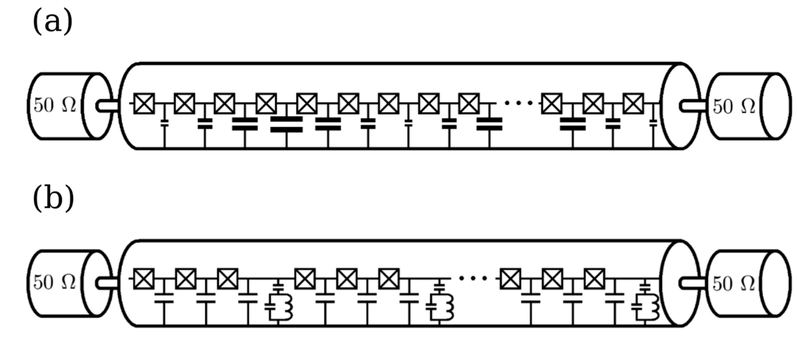


Figure 4: (a) Photonic crystal phase-matching (b) Resonant phase-matching

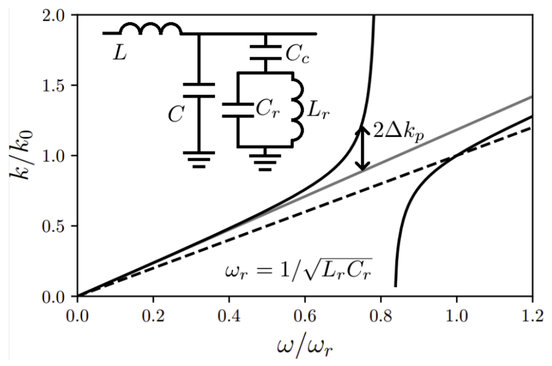


Figure 5: Dispersion of resonantly loaded transmission line. Pump near the resonance introduces mismatch Δk satisfying phase-matching condition. However, the dispersion also enables the propagation of unwanted sidebands, such as $\omega_p + \omega_s$, which degrades the amplifier's gain and bandwidth. The impedance is also modified by the resonance, leading to an impedance mismatch and causing reflections.

Numerical simulation setup

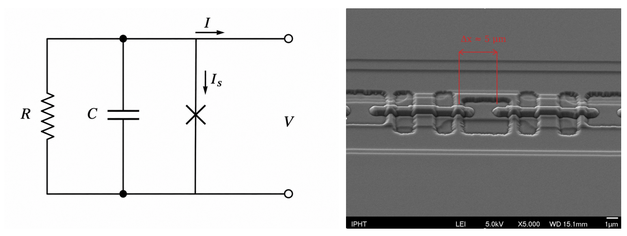


Figure 6: Lumped element model of RCSJ junction

$$C\frac{\Phi_0}{2\pi}\frac{d^2\varphi}{dt^2} + \frac{1}{R}\frac{\Phi_0}{2\pi}\frac{d\varphi}{dt} + I_c \sin(\varphi) = I_{\text{bias}}, \quad (5)$$

$$\Phi_0 = h/(2e), \dot{\varphi} = \frac{V}{\Phi_0}$$

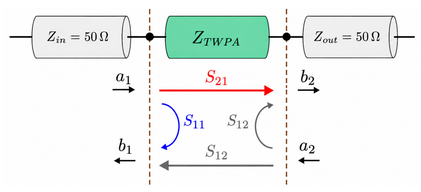


Figure 7: Schematic representation of a TWPA as a two-port microwave network.

Numerical simulators JoSIM and WRspice is used to solve such system and to calculate S_{21} and S_{11} :

$$S_{21} = \frac{b_2}{a_1} = \frac{V_{out} - R_{out} I_{out}}{V_{in} + R_{in} I_{in}}, S_{11} = \frac{b_1}{a_1} = \frac{V_{in} - R_{in} I_{in}}{V_{in} + R_{in} I_{in}}. \quad (6)$$

$$Gain = 20\log_{10}(|S_{21}|), Reflection = 20\log_{10}(|S_{11}|). \quad (7)$$

The goal is to make Gain > 15dB and Reflection < -10dB

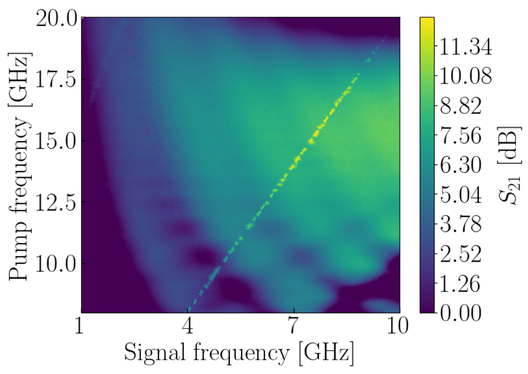


Figure 8: Example S_{21} as functions of the pump and signal frequencies for 3WM mixing case for homogenius TWPA.

Plasma resonance phase-matching and Third Harmonic Generation (THG) mediated gain in TWPA

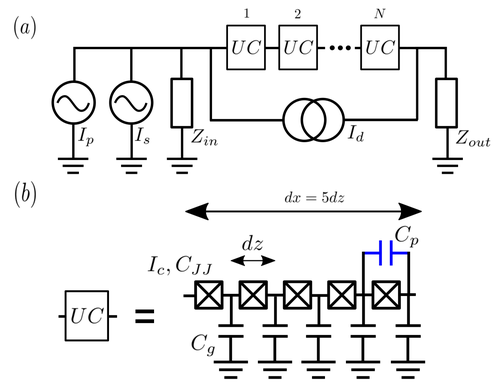


Figure 9: The shunting capacitance C_p of JJ shifts its plasma frequency into GHz range.In a periodic arrangement, the unique dispersion enables phase matching in PTWPA through THG.

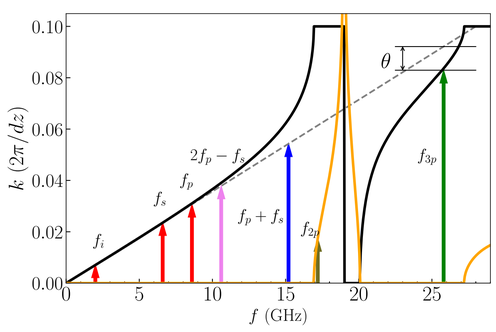


Figure 10: Black and orange curve are real and imaginary part of dispersion of the PTWPA calculated by ABCD matrix method. Dashed line is the linear approximation with additional phase shift for third harmonic. Dispersion enables effective phase-matching of the THG. Indicated modes are signal, idler, pump, third harmonic and sidebands.

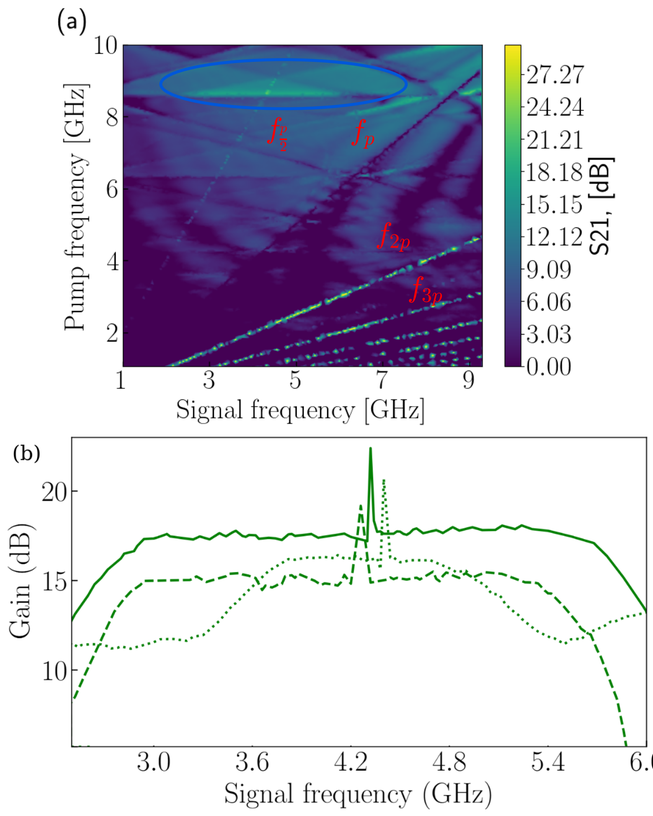


Figure 11: (a) Transmission colormapas functions of pump and signal frequency identify the optimal operating regime of the proposed TWPA (blue oval) and reveal efficient third-harmonic generation (THG), marked by f_{3p}. (b) Gain of the TWPA near the sweet spot. The highest gain occurs where THG is most efficient, a key feature of our TWPA design.



Figure 12: Current team who works on TWPA. From left to right: Dr. Kern, Dr. Neilinger, Dr. Rizvanov and Prof. Grajcar.

The main results of the previous project are:

- Identification of an amplification mechanism mediated by third-harmonic generation, demonstrating that a process commonly regarded as parasitic can enhance amplifier performance.
- Demonstration of high gain and phase matching through dispersion engineering involving a nearly linear dispersion region and the plasma cutoff. and analyzed.

The expected outcomes are:

- Further optimization of PTWPAs designs with respect to the fabrication possibilities of prefabrication center in Viena
- Identify suitable TWPA designs and operating parameters for optical photon-detection applications.
- Systematically characterize harmonic generation and its influence on gain and bandwidth in plasma-oscillation-based TWPAs operating in the 4WM regime.

Acknowledgements

This work was supported by the Slovak Research and Development Agency under contract No. APVV-25-0223 (Integrated Superconducting Photon Detectors). The authors thankfully acknowledges the Comenius University in Bratislava through the CLARA@UNIBA.SK high-performance computing facilities, services, and staff expertise at the Centre for Information Technologyand the computer resources at MareNostrum5 and the technical support provided by Barcelona Supercomputing Center (RES-FI-2025-1-0044). Part of the research results was obtained using the computational resources procured in the national project National competence centre for high performance computing (project code: 311070AKF2) funded by European Regional Development Fund, EU Structural Funds Informatization of society, Operational Program Integrated Infrastructure.

More information can be obtained from

- E. Rizvanov et al., J. Appl. Phys. 139, 074402 (2026).
- E. Rizvanov et al., J. Appl. Phys. 136, 174401 (2024).
- S. Kern et al., Phys. Rev. B 107, 174520 (2023).
- J. Delport et al., IEEE Trans. Appl. Supercond. 29, 5 (2019).
- S. R. Whiteley, IEEE Trans. Magn. 27, 2 (1991).

e-mail: emil.rizvanov@fmph.uniba.sk